



## Design and simulation of a smart ratiometric ASIC chip for VOC monitoring

Jesús García-Guzmán<sup>a</sup>, Nicola Ulivieri<sup>b</sup>, Marina Cole<sup>a,\*</sup>, Julian W. Gardner<sup>a</sup>

<sup>a</sup> School of Engineering, University of Warwick, Coventry CV4 7AL, UK

<sup>b</sup> Department of Information Engineering, Università di Siena, 53100 Siena, Italy

### Abstract

This paper reports on the design and simulation of a novel ratiometric application specific integrated circuit (ASIC) chip for the monitoring of volatile organic compounds (VOCs) or gases. The design integrates two polymeric chemoresistors in a ratiometric configuration, together with smart circuitry, into a single chip fabricated through a standard silicon CMOS process. The circuit provides automatic compensation of signal from variations in both supply voltage and ambient temperature. On-chip control of the operating temperature of the sensors is also an option. The response of the ratiometric set of polymeric chemoresistors to different concentrations of gases at different temperatures and humidities was simulated with the aid of a novel parametric Cadence model. Simulations confirm that the ratiometric configuration is less sensitive to temperature variations and that it also has a better performance in terms of humidity dependence when compared to an individual chemoresistor. These features, together with its ability to compensate for a large range in values of polymer resistance, make us believe that the circuit offers relevant smart capabilities at a very low-cost and so it can be used as the main component for the mass production of a self-calibrating, programmable, palm-top instrument.

© 2003 Published by Elsevier Science B.V.

**Keywords:** Smart sensor; ASIC; Resistive gas sensor; Ratiometric sensor array; Behavioural models

### 1. Introduction

Further advances, in the field of polymer resistors for the sensing of vapours, require the development of low-cost smart devices capable of addressing the problems of both process variation and changes in environmental conditions. The use of integrated circuits capable of self-calibration and compensation within a single chip unit can provide a good solution. The adoption of a standard fabrication process allows the integration of smart interface circuitry and arrays of polymer-based sensors, leading to the development of novel intelligent sensor systems for gas or vapour monitoring.

Some of the problems associated with conducting polymers, such as temperature dependence, have already been addressed through the design of four- and five-element microbridge devices [1–3] and a significant reduction in the values of temperature and humidity coefficients was achieved.

In this paper we describe an application specific integrated circuit (ASIC) chip for gas monitoring that provides several

smart features and incorporates a pair of polymer resistors in a ratiometric configuration [4]. In order to perform detailed analyses of the behaviour of this ratiometric chip, a parametric model was developed to simulate the polymer resistance on exposure to a given gas at different temperatures and humidities [5]. This model is particularly useful because it permits the response of polymeric chemoresistors to be predicted before CMOS processing. Cadence software was used for the design and simulation of the ASIC chip as well as for the implementation of the model. An Alcatel 0.7  $\mu\text{m}$  CMOS process was chosen for the design and fabrication of the chip through the low-cost Europractice scheme.

### 2. Description of the design

Fig. 1 shows the overall structure of the new smart gas sensor system. The main component is the ASIC chip, which performs two basic functions: (a) sensing the gas presence and concentration and (b) controlling the operating temperature of the gas sensor. Within the ASIC chip, the top section corresponds to the gas sensor circuit, whereas the bottom sections correspond to temperature control and monitoring. A microcontroller unit is used for processing the inputs and

\* Corresponding author. Fax: +44-1203-418922.  
E-mail address: mvc@eng.warwick.ac.uk (M. Cole).  
URL: http://www.eng.warwick.ac.uk/srl.

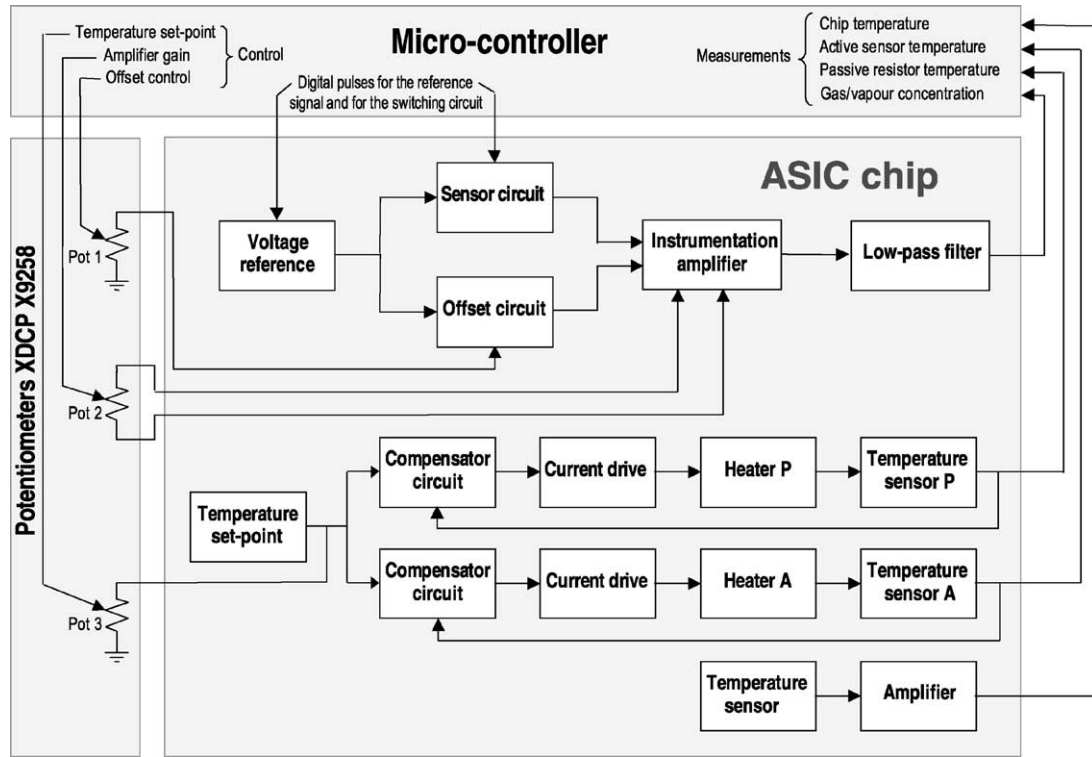


Fig. 1. Top representation of the ratiometric sensor system.

63 outputs of the ASIC chip. Additionally, three digitally controlled  
 64 potentiometers (available in the Xicor's X9258 integrated circuit)  
 65 are used in order to accomplish some specific trimming functions.  
 66

2.1. Gas sensor section

The first section of the ASIC chip is the circuit that includes two polymeric sensing resistors in a ratiometric con-

Table 1  
 Model parameters used in the simulations

Parameter used in the Cadence model	Value(s) <sup>a</sup>	Symbols used for Cadence parameters in the Eq. (1)	Description
$C_{gas}$	1k	$C_G$	Gas concentration (ppm)
Humid	0–30k	$C_H$	Humidity concentration (ppm)
Temper	40–100	$T$	Sensor temperature (°C)
$K_{sH}$	31.32	$K_{sH}$	Temperature coefficient for the humidity (°C)
$k_H$	−94n	$k_H$	Sensitivity coefficient for the humidity (1/ppm)
$\gamma_{H}$	1	$\gamma_H$	Power low exponent for the humidity
Slope	1	–	Slope of the flicker noise ( $1/f^{slope}$ )
Vol	$30 \times 10^{-15}$	–	Polymer volume (m <sup>3</sup> )
X	$300 \times 10^{-27}$	–	Polymer coefficient to evaluate flicker noise
SDS.Ct	−1	–	SDS control (positive → active, negative → inactive)
w1SDS.off	–	–	Pole for off-dynamics SDS
w1SDS.on	–	–	Pole for on-dynamics SDS
w2.on	10k	–	Second pole on-dynamics chemical transient
w2.off	4k	–	Second pole off-dynamics chemical transient
w1.on	10m	–	First pole on-dynamics chemical transient
w1.off	4m	–	First pole off-dynamics chemical transient
$R_0$	9512	$R_{SC0}$	Sensor baseline resistance (Ω)
B	2	B	Temperature coefficient for sensor baseline resistance (°C)
$K_s$	88.42	$K_{sG}$	Temperature coefficient for the gas (°C)
$k_1$	3.2μ	$k_G$	Sensitivity coefficient for the gas (1/ppm)
gamma	1.07	$\gamma_G$	Power low exponent for the gas

<sup>a</sup> The values of the parameters used for simulations are obtained from measurements on carbon-black polymer film performed at the Sensors Research Laboratory of the University of Warwick with exception of the noise measurements which were performed by University of Torvegata (Rome).

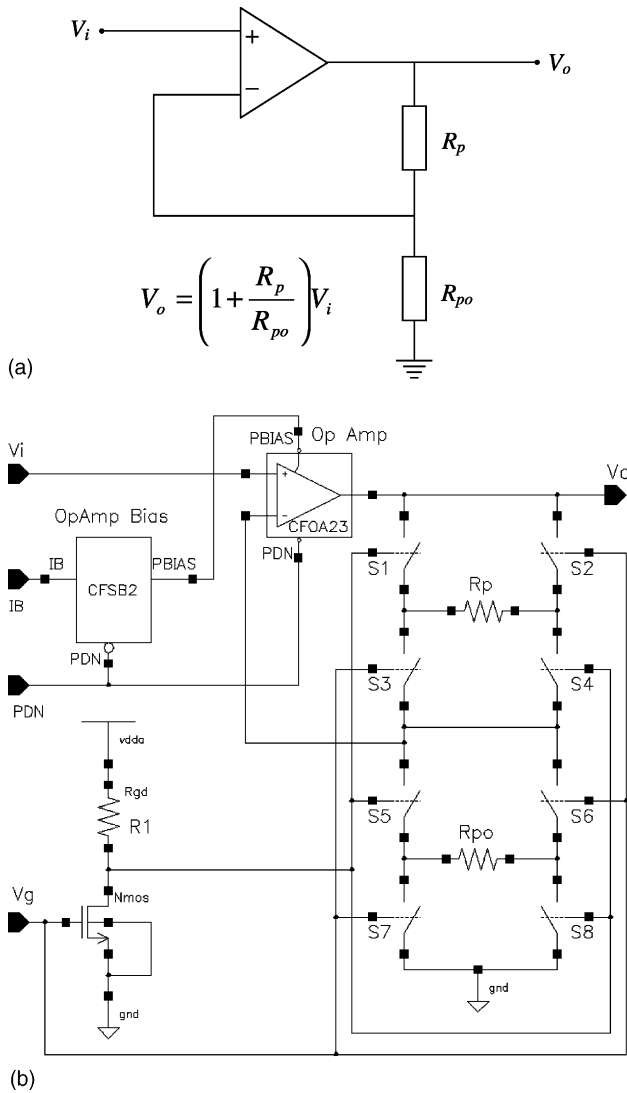


Fig. 2. Ratiometric sensor circuit: (a) basic principle; (b) Cadence implementation including analogue switching.

figuration for the monitoring of gases. The basic operating principle of ratiometric configuration is shown in Fig. 2(a). In this, two sensors are connected in a non-inverting operational amplifier configuration. One of the sensors  $R_p$ , is exposed to gas whilst the second one  $R_{po}$ , is passivated with an inert material, such as Nafion, which also offers common mode rejection of humidity signals, reduces the temperature sensitivity of the responses and produces an increase in response with an increase in temperature. When exposed to the presence of gases, the electrical resistance of the active polymer element changes, giving an indication of the concentration of the gas, whilst any common mode effects, such as aging, temperature dependence and humidity dependence, will cancel each other through the simple ratio  $R_p/R_{po}$ .

The gas microsensors are constructed by spray-coating a polymer across the aluminium electrodes. The electrodes are fabricated in a CMOS process, with the subsequent steps of

polymer deposition and passive coating completing the fabrication of the active and passive chemoresistors. The actual behaviour of these resistors cannot be precisely predicted. It is known from previous research [1–3,6,7] that the polymer resistance will vary in the presence of gases, but there are several factors which affect these variations, e.g. temperature, humidity, ageing, and applied voltage. Even the actual resistance value of the devices is not easily controllable during the deposition process and significant differences appear between resistors fabricated through apparently identical batches.

Consequently, the structure of the gas sensor circuit was designed to overcome these problems. Firstly, a ratiometric pair of polymer resistors is used in order to provide at least partial cancellation of the above-mentioned variations. Secondly, the polymeric sensors are excited through the use of circuitry that also reduces these effects. Finally, smart circuitry is added for the self-cancellation of offset errors for the calibration of the device. As a result, the gas sensor circuit produces an amplified and filtered voltage signal proportional to the change in resistance experienced by one of the polymer resistors on gas exposure while the other resistor is used as a passive reference.

The blocks in the top section of the ASIC chip diagram in Fig. 1 perform this sensing function. A reference pulsed voltage signal is sent to a pair of ratiometric circuits. The first of these is the sensor circuit, whose schematic view is shown in Fig. 2(b). The polymer resistors  $R_p$  and  $R_{po}$  are connected, as described before, to an operational amplifier in a non-inverting configuration, following basically the same ratiometric principle reported previously [4]. In this,  $R_p$  is the active sensor exposed to the gas, while  $R_{po}$  remains passive. Apart from the elimination of temperature, humidity, and aging effects on the baseline resistance, the sensor circuit also incorporates polarity pulse switching in order to cancel long-term drift problems caused by the polarisation effect. The FET-based switches S1 to S8, controlled through pulses applied to the input  $V_g$ , invert alternately the voltage at the terminals of  $R_p$  and  $R_{po}$ , providing compensation against any polarisation effect or drifting associated

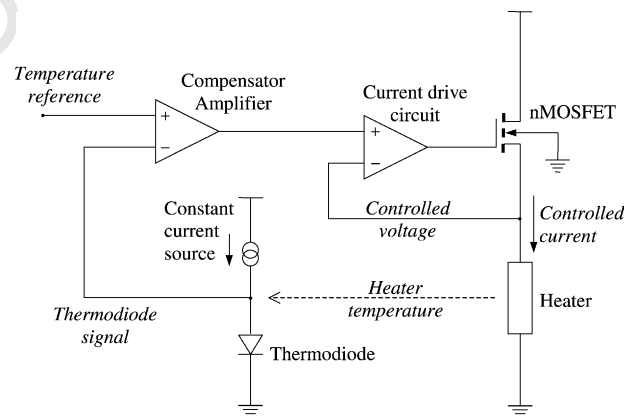


Fig. 3. Simplified schematic diagram of the temperature control circuit.

126 with a constant dc voltage. The benefits obtained with the  
 127 ratiometric configuration of the sensors were confirmed via  
 128 simulations as described below.

129 The second ratiometric circuit is used to offset the output  
 130 signal of the sensor ratiometric circuit under non-exposure  
 131 circumstances, thus removing any variation in the polymer  
 132 resistance ratio from unity. This offset signal is digitally ad-  
 133 justed through the external potentiometer *Pot 1* (Fig. 1). The  
 134 outputs of both ratiometric circuits are fed into an instru-  
 135 mentation amplifier in which any difference between the in-  
 136 put signals will cause an output approximately proportional

137 to the concentration of the monitored gas. The signal is then  
 138 adjusted with the aid of the potentiometer *Pot 2*, which sets  
 139 the gain of the amplifier. Finally, a Bessel low-pass filter  
 140 was found to be the most suitable to remove high frequency  
 141 switching errors from the amplified signal (Table 1).

2.2. Temperature control section 142

143 The second major task to be performed by the ASIC chip  
 144 is the control of temperature, which is known to seriously  
 affect the response of polymer sensors [1–3,6,7]. The bot-

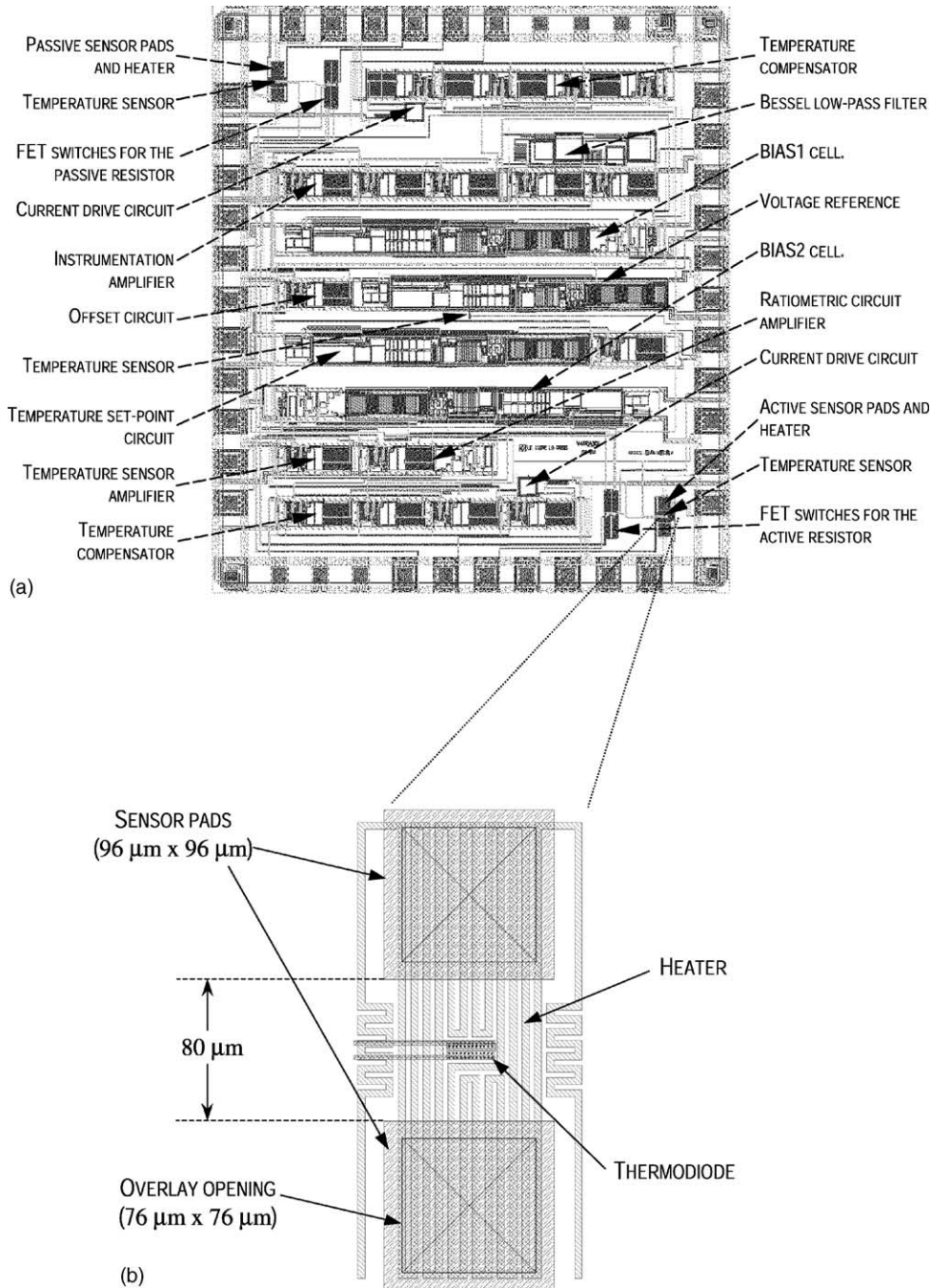


Fig. 4. Layout view of (a) the complete smart ratiometric ASIC chip and (b) the sensor area including heater and thermodiode.

145 tom sections on the ASIC chip diagram in Fig. 1 correspond  
 146 to this control and monitoring function. In order to maintain  
 147 the proper operating conditions and to minimise variations,  
 148 a controlled heater is placed underneath the electrodes of  
 149 each polymer resistor. A temperature sensor closes the con-  
 150 trol loop by feeding back a signal to the compensator circuit,  
 151 where it is compared with a reference point that is set with  
 152 the aid of a third external potentiometer. Here, a differen-  
 153 tial amplifier produces a compensating signal proportional  
 154 to the difference of temperatures between the heater and  
 155 the set point. This compensating signal controls the current  
 156 through the heaters thus in turn controlling the temperature  
 157 of the polymer resistors. A simplified schematic diagram of  
 158 the temperature control section is shown in Fig. 3. An ad-  
 159 ditional temperature sensor, whose output is amplified, is  
 160 used to monitor the ambient temperature of the chip. The  
 161 outputs of the temperature sensors are made available to the  
 162 microcontroller unit.

### 163 2.3. Layout view

164 The layout view for the chip, shown complete in Fig. 4(a),  
 165 was drawn with the *Virtuoso* layout editor according to the  
 166 specifications and layout rules of the Alcatel Microelectron-

167 ics 0.7  $\mu\text{m}$  CMOS technology. The dimensions of the ASIC  
 168 chip are  $3300 \mu\text{m} \times 3750 \mu\text{m}$  and it contains all the compo-  
 169 nents that are represented in the block diagram of Fig. 1. The  
 170 cells are placed along several rows in the layout, thus ob-  
 171 taining a symmetrical distribution with the two gas sensors  
 172 located at opposite corners of the chip, to aid post-CMOS  
 173 polymer deposition.

174 The sensor area of the layout is shown in Fig. 4(b). The  
 175 electrodes, in metal 2 layer, are  $96 \mu\text{m} \times 96 \mu\text{m}$  in size,  
 176 with  $80 \mu\text{m}$  interelectrode gap, in order to achieve approx-  
 177 imately  $10 \text{ k}\Omega$  resistance when using carbon-black poly-  
 178 mer composite films [8]. The heaters are constructed un-  
 179 derneath the electrodes in the metal 1 layer, which has a  
 180 nominal sheet resistance of  $50 \text{ m}\Omega/\text{sq}$ . Each heater has a  
 181 nominal design resistance of  $50 \Omega$ . The thermodiodes are  
 182 placed in the centre of the heater regions, just between the  
 183 electrodes.

184 The cells *Bias1* and *Bias2* provide the bias current for  
 185 the operational amplifiers according to the bias strategy re-  
 186 quired by the Alcatel analogue cells and they also supply the  
 187 current for the driving of the temperature sensors. Several  
 188 test points are available at the bonding pads for testing pur-  
 189 poses, allowing the realisation of measurements at different  
 190 sections of the circuit.

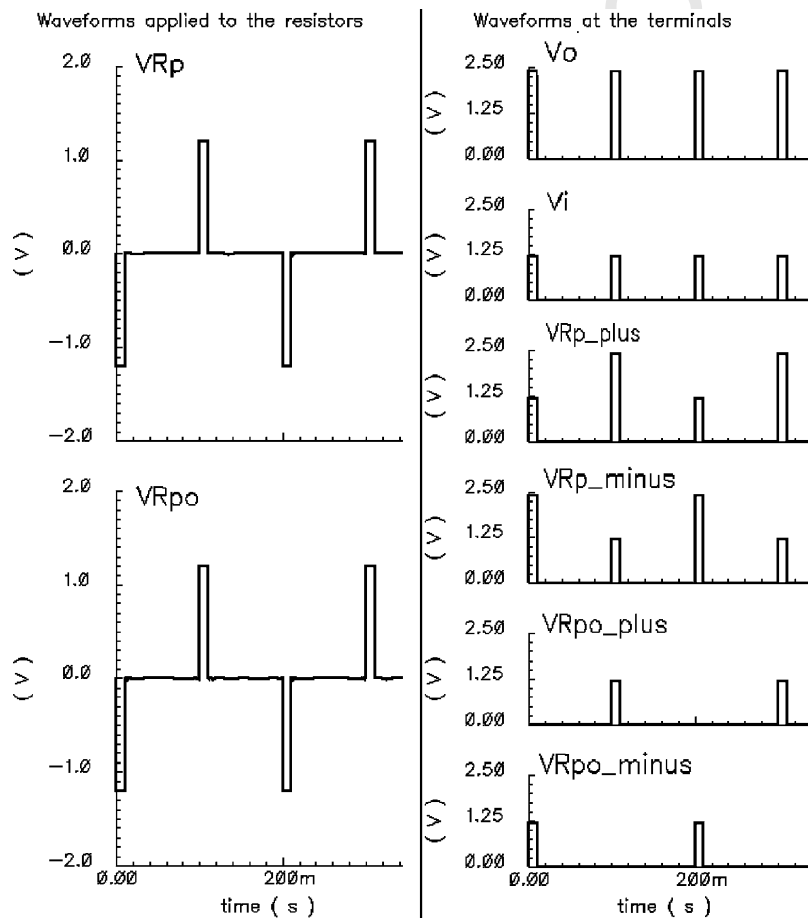


Fig. 5. Simulation of sensor voltages in the circuit.

191 A number of tests were performed with the *Diva* and  
 192 *Dracula* software packages in order to check the consistency  
 193 of the design with the layout rules, with the electrical  
 194 rules and with the substrate requirements under the particular  
 195 CMOS process selected for the fabrication of the ASIC  
 196 chip. In order to obtain the openings down to metal 2 layer  
 197 for the deposition of the polymers onto the sensor electrodes,  
 198 it was necessary to include some special modifications while  
 199 still following the standard CMOS process.

### 200 3. Simulations

201 The *Spectre* simulator was used to test each part of the  
 202 design. Fig. 5 shows the voltages obtained at the ratiometric  
 203 sensor circuit when assuming initially equal resistances  
 204 for  $R_p$  and  $R_{po}$  and hence disregarding any variations due  
 205 to exposure to reactive gases. The left plots correspond to  
 206 the actual voltage waveforms at the terminals of the resistors,  
 207 i.e. the differences in the corresponding positive voltages,  
 208 plotted on the right, appearing at the *plus* and *minus*  
 209 terminals of each resistor. The simulation results confirm

210 the advantage of using the switching circuitry in order to  
 211 invert the sign of the voltages at the chemoresistors terminals  
 212 and thus providing compensation against polarisation  
 213 effects.

214 Fig. 6 shows the voltage waveforms appearing at every  
 215 stage of the gas sensor section. The reference signal  $V_{ref}$   
 216 (Fig. 6(a)) produced by feeding pulses to a standard bandgap  
 217 cell consists of pulses that are 10 ms in width and have an  
 218 amplitude of 1.2 V. This signal produces the response that  
 219 is registered at the output of the offset circuit (Fig. 6(c)),  
 220 which is calibrated to the baseline signal, i.e. the sensors  
 221 unexposed to gases. After calibration, exposure to gases is  
 222 simulated via the change in resistance  $\delta$  applied to the active  
 223 sensor. The sensor output  $V_{sensor}$  (Fig. 6(b)) differs from the  
 224 offset signal  $V_{offset}$  and the difference in voltage is applied  
 225 to the input of the instrumentation amplifier. This differential  
 226 voltage  $V_{diff}$  (Fig. 6(d)) was only 60.37 mV in the simulation  
 227 when the change in resistance  $\delta$  was set to 0.05, i.e. 5% of  
 228  $R_{po}$ . When the gain of the amplifier is set to 50, the amplitude  
 229 of the signal is raised to approximately 3 V in amplitude  
 230 ( $V_{amp}$ , Fig. 6(e)). Finally,  $V_{out}$  represents the filtered signal  
 231 at the output of the circuit (Fig. 6(f)).

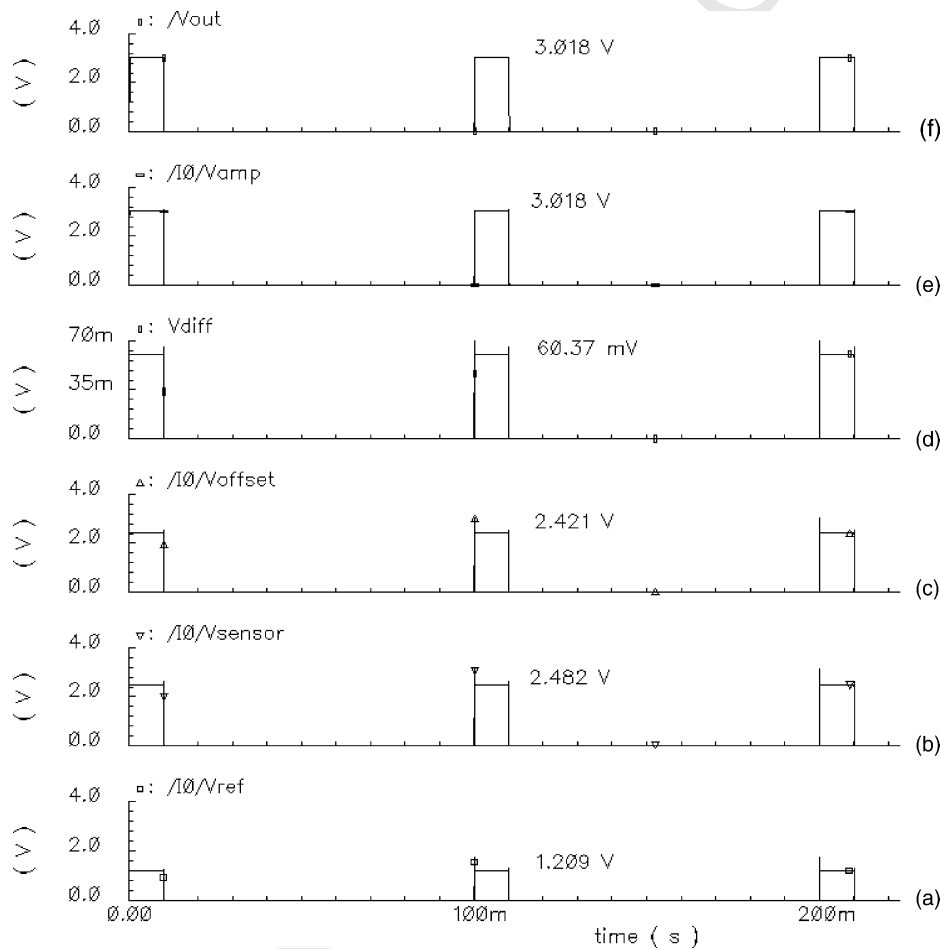


Fig. 6. Voltage simulation with a change in resistance equal to 5% of  $R_{po}$ : (a) reference voltage, (b) voltage at the output of the sensor circuit, (c) offset voltage, (d) differential input at the instrumentation amplifier, (e) amplified voltage, and (f) output of the low-pass filter.

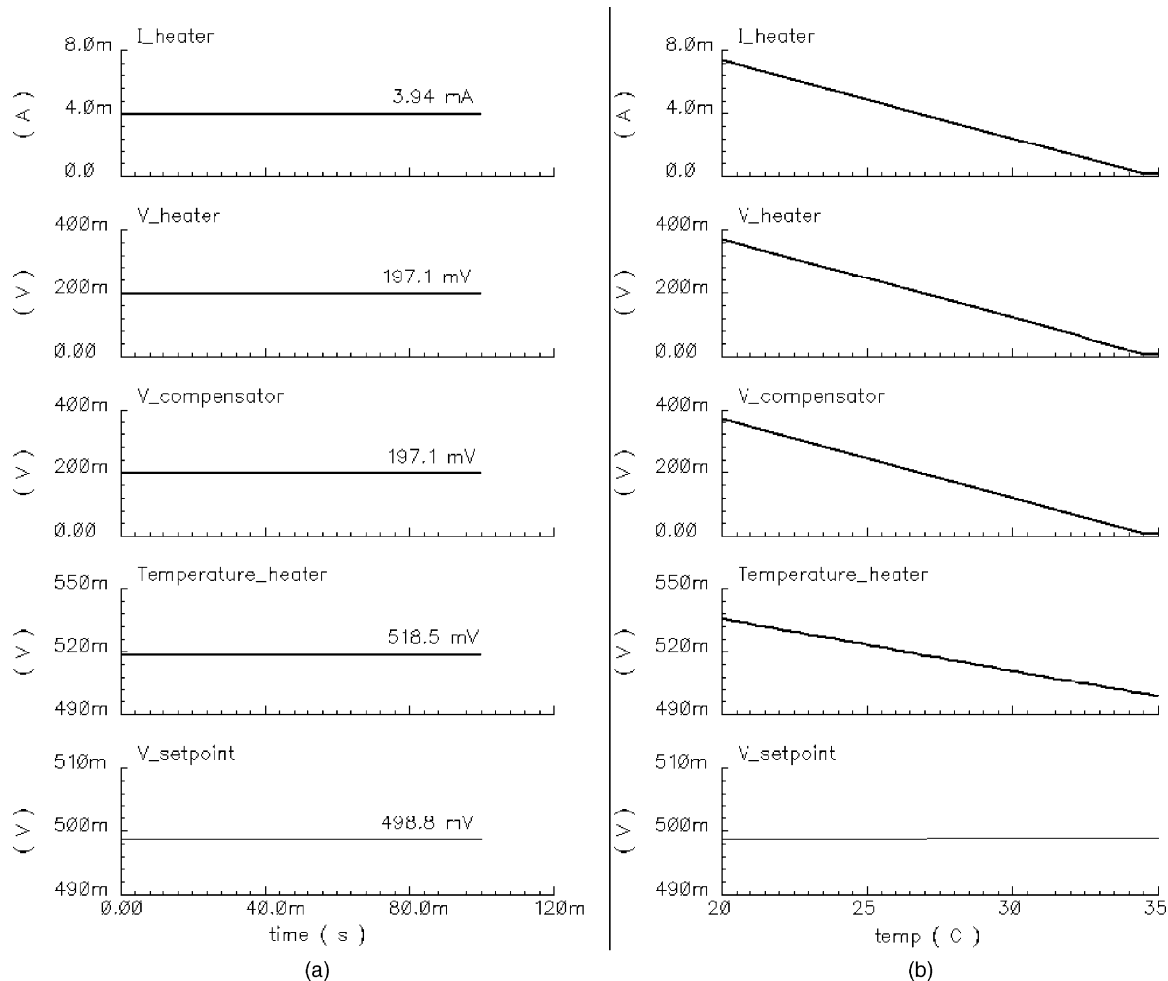


Fig. 7. Waveforms for the temperature control system: (a) results at 27°C, (b) response between 20 and 35°C.

232 The performance of the temperature control section was  
 233 also simulated. Fig. 7(a) shows the voltages obtained at  
 234 27°C, whereas Fig. 7(b) shows the voltage waveforms re-  
 235 sulting when temperature varies between 20°C and a nomi-  
 236 nal setpoint at 35°C.

237 Further simulations also showed that the circuit is capable  
 238 of dealing with the wide range in the actual resistance ob-  
 239 tained for the different types of polymer sensors (e.g. three  
 240 orders of magnitude).

### 241 3.1. Application of the polymeric chemoresistor model

242 In order to compare performances of ratiometric config-  
 243 uration to discrete chemoresistors, the polymeric chemore-  
 244 sistor model was used. This model, implemented in Ca-  
 245 dence and described thoroughly elsewhere [5], is able to  
 246 simulate accurately the polymeric chemoresistor response to  
 247 gas and humidity under different operating conditions. The  
 248 model simulates the static and dynamic sensor response to  
 249 gas or gas mixture exposure, and includes flicker and John-  
 250 son noise. It also takes account of the sensor sample de-  
 251 livery system. Fig. 8(a) shows the conceptual structure of

the proposed model having three inputs ( $C_G$ ,  $C_H$ ,  $T$ ) for gas 252  
 and humidity concentration and sensor temperature, and two 253  
 pins ( $R_+$ ,  $R_-$ ) for sensor connection with the rest of the 254  
 circuitry. The inputs are connected to voltage sources whose 255  
 voltage level emulates both the gas and humidity concentra- 256  
 tions (1 V  $\leftrightarrow$  1 ppm) and the sensor temperature (1 V  $\leftrightarrow$  257  
 1°C). The model has been implemented as a standard cell 258  
 (SC) in Cadence software (Fig. 8(b)). The polymeric sensor 259  
 is represented as a complex impedance  $Z_{SC}$ , with two 260  
 noise sources in series (thermal and flicker noise [8]).  $Z_{SC}$  261  
 is the impedance resulting from the parallel combination of 262  
 the sensor capacitance  $C_{SC}$  and the sensor resistance  $R_{SC}$ . 263  
 Parasitic resistances and capacitances are neglected because 264  
 they are insignificant when compared with  $R_{SC}$  and  $C_{SC}$  [5]. 265

The sensor static response is a function of the gas concentra- 266  
 tion  $C_G$ , the sensor temperature  $T$  and the water vapour 267  
 concentration  $C_H$ , while the dynamic response depends both 268  
 on the gas transfer method and/or on the gas reaction kinet- 269  
 ics. The static resistance of the SC,  $R_{SC}$ , is evaluated in the 270  
 block 'Sensor Static Response' (see Fig. 8(a)) which imple- 271  
 ments the developed model, assuming that carbon-black 272  
 composite polymer films are used as gas sensitive materials. 273

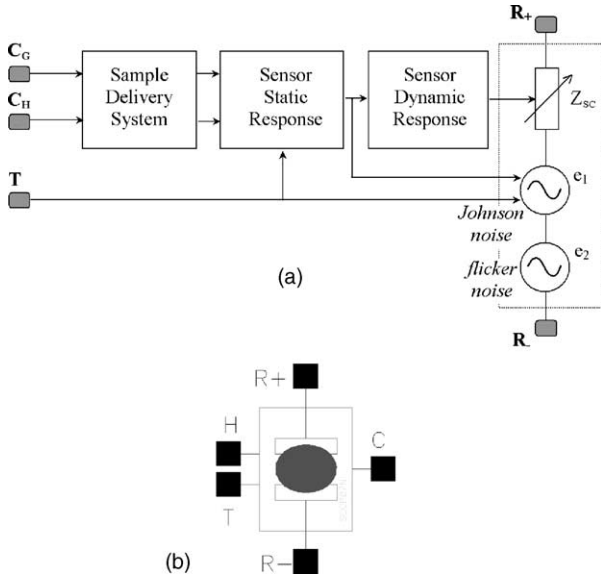


Fig. 8. (a) Model framework of the SC for a polymeric gas sensor. (b) symbol for the cell.

274 The model developed for these materials in Ref. [5] has been  
 275 expanded in order to include the temperature variations of  
 276 the baseline resistance and the static resistance is given by

$$R_{SC} = R_{SC0} \exp\left(\frac{B}{T}\right) \times \left[ 1 + k_G C_G^{\gamma_G} \exp\left(\frac{K_{sG}}{T}\right) + k_H C_H^{\gamma_H} \exp\left(\frac{K_{sH}}{T}\right) \right] \quad (1)$$

281 where  $R_{SC0}$  is the baseline sensor resistance (measured in  
 282 presence of a reference gas, generally synthetic air or nitro-  
 283 gen),  $k_G$  and  $k_H$  are sensitivity coefficients,  $C_G$  and  $C_H$   
 284 are the gas/vapour concentrations expressed in ppm,  $\gamma_G$  and  $\gamma_H$   
 285 are the power law exponents,  $B$ ,  $K_{sG}$  and  $K_{sH}$  are the temper-  
 286 ature coefficients, and  $T$  the temperature in Kelvin. The sub-  
 287 scripts G and H refer to the gas and the water vapour, respec-  
 288 tively. The sensitivity coefficients can be positive or negative  
 289 depending on the nature of the gas and the polymer, produ-  
 290 cing an increase or decrease of the sensor resistance after  
 291 the gas injection. The transient behaviour of the polymeric  
 292 gas sensor is simulated by a second-order multi-exponential  
 293 model implemented through a second-order low-pass filter  
 294 ('Sensor Dynamic Response' in Fig. 8(a)). Since the  
 295 on-dynamics are generally faster than the off-dynamics, two  
 296 filters with different poles have been used. The sample deli-  
 297 very system is also modelled ('Sample Delivery System'  
 298 in Fig. 8(a)) in order to include the real gas transfer [5].

299 The general parametric model described above was used  
 300 to simulate the response of the polymeric chemoresistors  
 301 in the ratiometric configuration. Fig. 9 shows how the cells  
 302  $SC_a$  and  $SC_p$  were used to represent the active and passive  
 303 sensors.

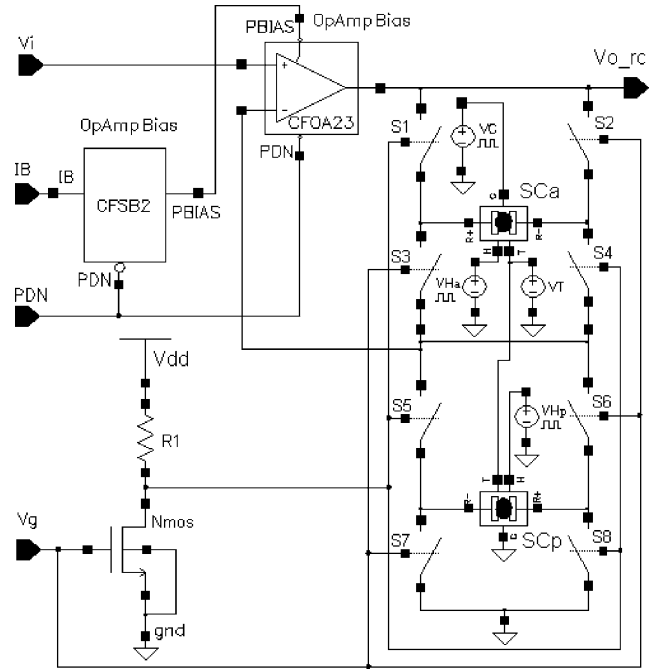


Fig. 9. Ratiometric sensor circuit. The sensor cell  $SC_a$  emulates the behaviour of the active polymeric sensor, while the cell  $SC_p$  mimics the passive sensor.

304 Two passivation methods were tested in the simulations.  
 305 In the first case, represented in Fig. 10(a), one of the poly-  
 306 meric sensors is coated with an inert material to avoid the  
 307 gas effect. In this way, the passive sensor is sensitive to tem-  
 308 perature variation but it does not respond to the gas or ambi-  
 309 ent humidity. The water vapour concentration is fixed to the  
 310 concentration present at the moment of the coat deposition  
 311 (e.g. RH = 40% at 20 °C corresponding to 9214 ppm). The  
 312 gas flow is split in two paths to expose both sensors. The  
 313 passivation was simulated by connecting the input 'C' of the  
 314  $SC_p$  cell to gnd (gas concentration = 0 ppm) and the input

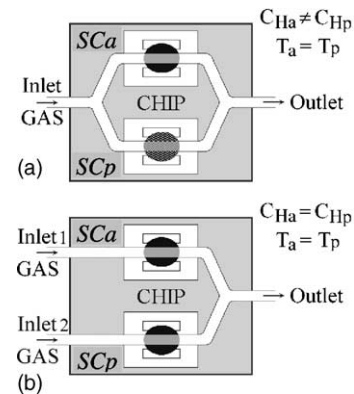


Fig. 10. The use of the reference sensor  $SC_p$  in the ASIC chip: (a) the polymer sensor  $SC_p$  is coated with an inert material to avoid the reaction with a gas which flow over sensors  $SC_a$  and  $SC_p$ ; (b) two separate flow paths are used to expose the two sensors to different gases but to the same water vapour concentration; this enables for humidity rejection.



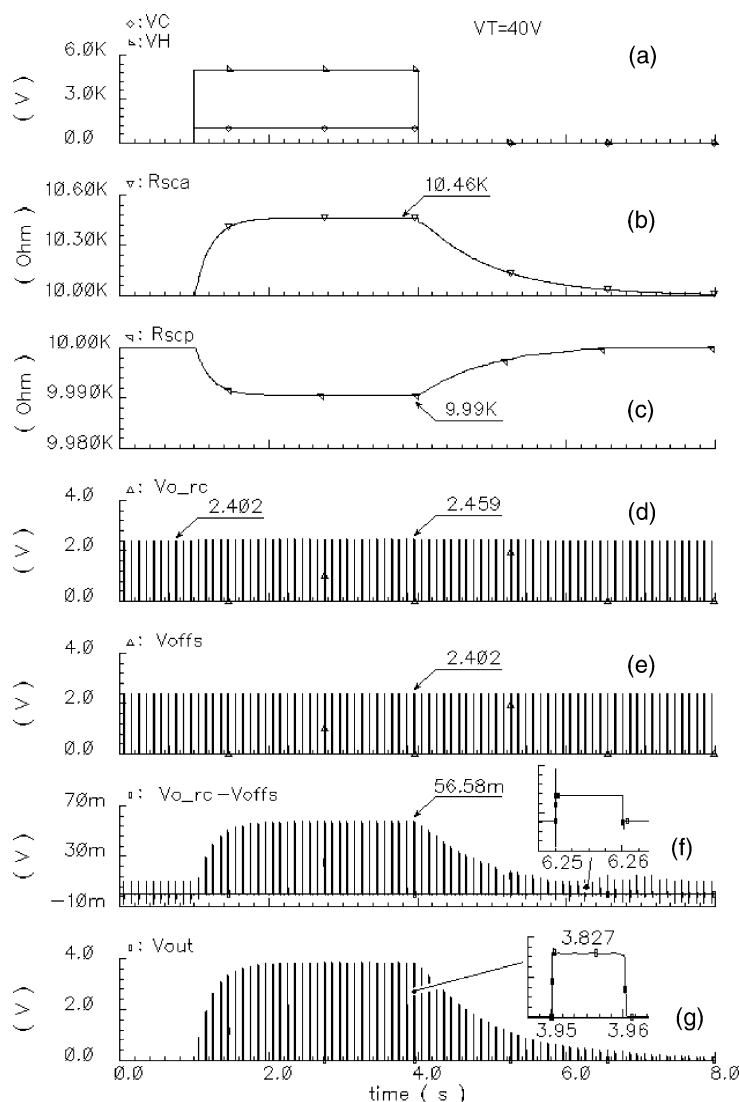


Fig. 11. Transient analysis of the ratiometric circuit for active and passive baseline resistances of  $10\text{ k}\Omega$  at  $40^\circ\text{C}$ , gas concentration = 1000 ppm, water vapour mixed to the gas = 5000 ppm: (a) voltage pulses applied to the sensor cell  $SC_a$  simulating the humidity and gas concentration ( $1\text{ V} \leftrightarrow 1\text{ ppm}$ ); (b) resistance of the active sensor; (c) resistance of the passive sensor; (d) output voltage of the ratiometric circuit; (e) output voltage of the offset circuit; (f) differential input of the instrumentation amplifier; (g) output of the gas sensor section.

315 'H' to a voltage source (e.g.  $VH_p = 9214\text{ V} \rightarrow 9214\text{ ppm}$ ).

316 The second method requires two separate inlets to carry  
 317 the gas under test and a reference gas to the sensors  $SC_a$  and  
 318  $SC_p$  (Fig. 10(b)). In this case the sensor  $SC_p$  is not coated  
 319 but it acts as a reference device because the reference gas  
 320 is injected in the second inlet ('Inlet 2 GAS'). This solution  
 321 allows cancelling the humidity effect, when the reference  
 322 gas has the same water vapour concentration as the gas under  
 323 test injected in the 'Inlet 1 GAS'.

324 Fig. 11 shows the results of simulations performed using  
 325 polymer resistors of  $10\text{ k}\Omega$  at  $40^\circ\text{C}$  under the second pas-  
 326 sivation method. Gas and humidity concentrations of 1000  
 327 and 5000 ppm, respectively were applied to the sensors ter-  
 328 minals. The changes in resistances of active and passive  
 329 sensors are shown in Fig. 11(b) and (c). The output signals  
 330 from ratiometric and offset sections are also shown. The

331 differential input to the amplifier is depicted in Fig. 11(f)  
 332 and the output signal of the gas sensor section is shown in  
 333 Fig. 11(g).

334 The benefits of the ratiometric circuit structure are com-  
 335 pared to the potential divider configuration (Fig. 12) already  
 336 discussed elsewhere [5]. In particular, the temperature and  
 337 humidity dependencies of the circuits are explored.

338 Figs. 13 and 14 show the percentage variation of the cir-  
 339 cuit output voltage with varying sensor temperature and hu-  
 340 midity. The two setups depicted in Fig. 10 are taken into  
 341 account. The ratiometric configuration shows less sensitiv-  
 342 ity to temperature variation compared to the discrete circuit.  
 343 In particular, the baseline output value is not sensitive to  
 344 the temperature variation when the configuration with refer-  
 345 ence gas shown in Fig. 10(b) is adopted. These results can  
 346 be observed in the curves for the ratiometric circuit with

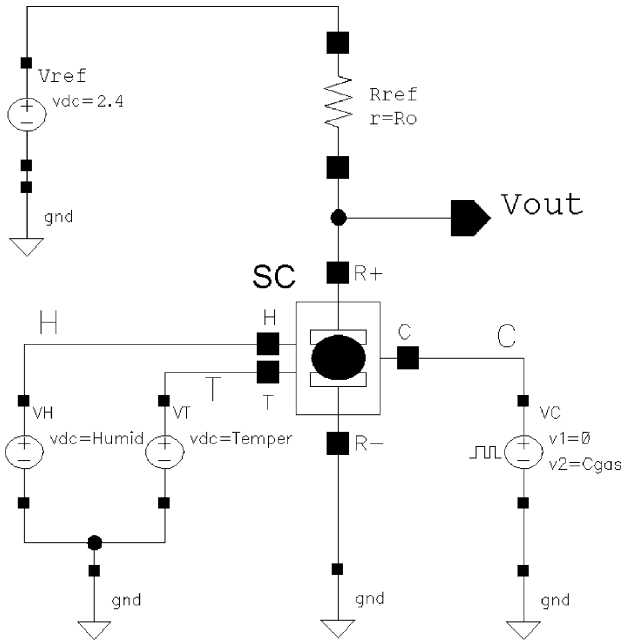


Fig. 12. Schematic view of the single chemosensor circuit.

$C_{Ha} = C_{Hp}$ , depicted in Fig. 13(a) and (b). This is expected, since the sensors are fabricated under the same conditions and they should respond to temperature changes with the same exponential law. The plots in Fig. 13(c) and (d) show that the ratiometric circuit has superior performance when compared to a single chemosensor circuit exposed to gas at varying temperature.

The ratiometric circuit shows better performance also in terms of linear humidity dependence (Fig. 14). The water vapour effect is cancelled by the reference sensor  $SC_p$  when this one is not coated and the configuration depicted in Fig. 10(b) is adopted ( $C_{Ha} = C_{Hp}$ ). If the reference sensor  $SC_p$  is coated with an inert material, as in Fig. 10(a), the humidity effect cannot be annulled (ratiometric curves for  $C_{Ha} \neq C_{Hp}$  in Fig. 14) but the ratiometric circuit is still less sensitive with respect to the potential divider configuration.

Noise simulation was also performed based on the model developed in Ref. [5]. Fig. 15 shows the simulated noise analysis of the ratiometric circuit. The operational amplifier CFOA23 (Fig. 9) gives the main contribution to the total output noise. The polymeric sensor noise is also shown and it is assumed to be dominated by flicker noise measured for polymer carbon films [8]. The RMS value of the noise volt-

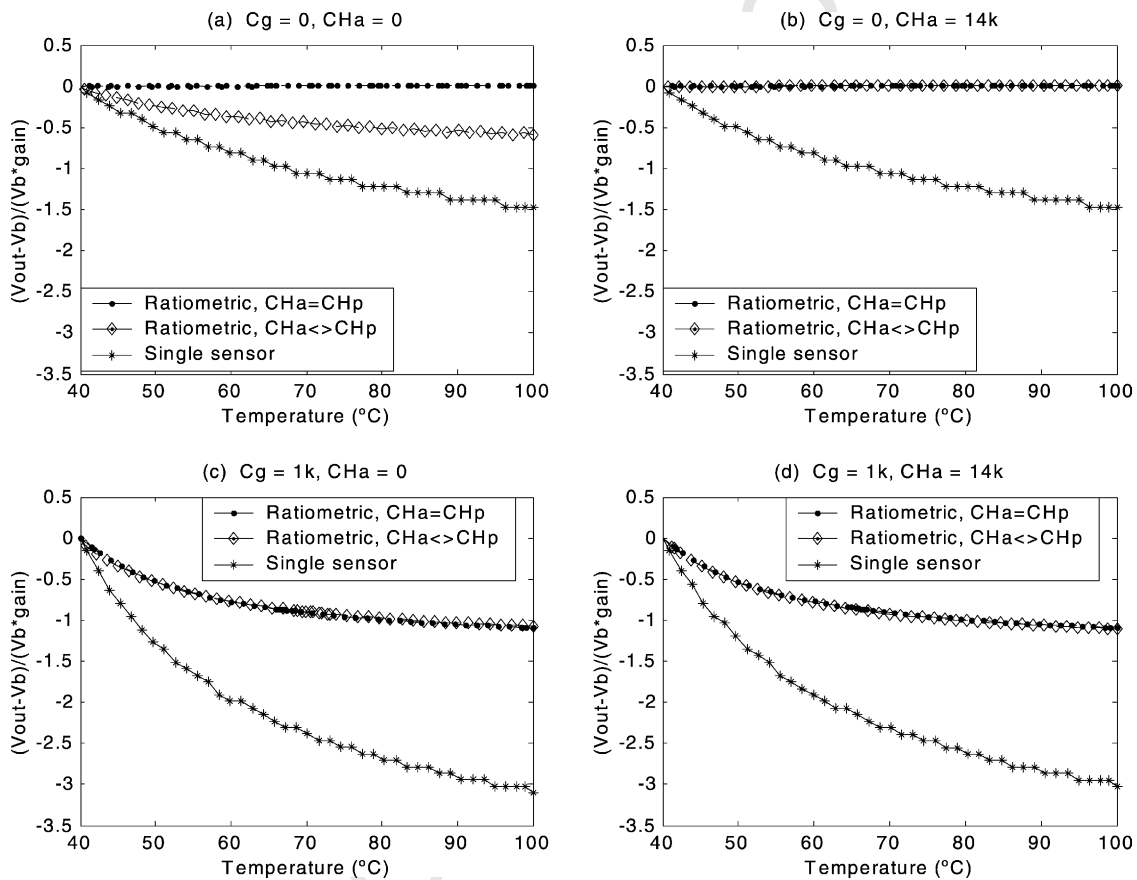


Fig. 13. Percentage variation of the output voltage for the ratiometric and potential divider circuits when the temperature of the sensors spans from 40 to 100 °C: (a) response to gas and water vapour concentrations equal to zero; (b) response with wet air and without gas exposure; (c) response to gas exposure with dry air; (d) response with gas exposure and wet air.

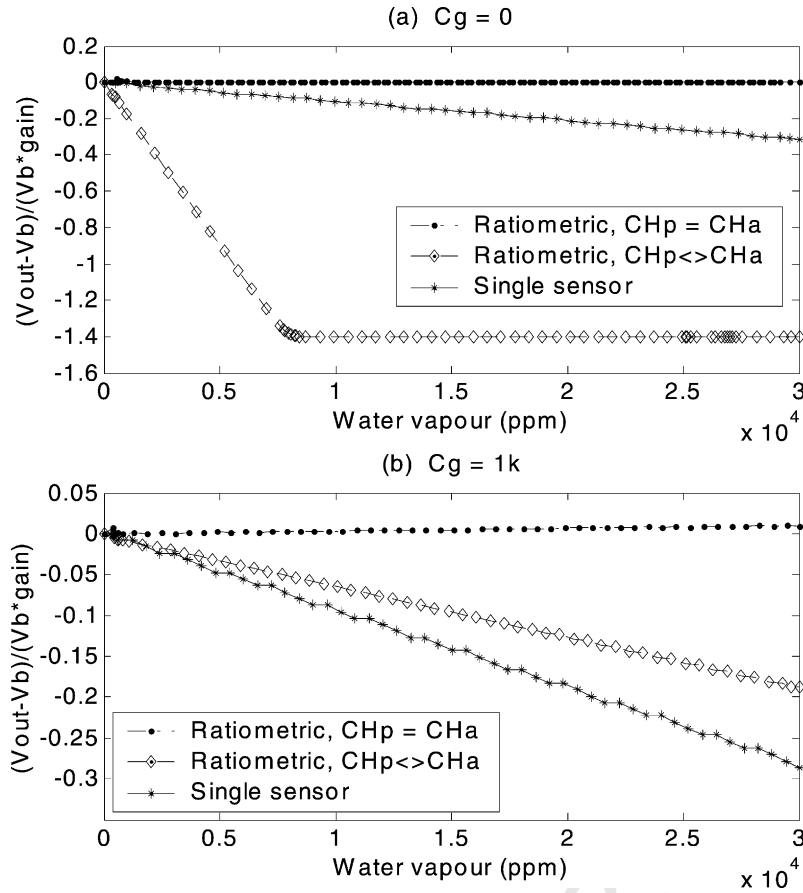


Fig. 14. Percentage variation of the output voltage for the ratiometric and potential divider circuits when the water vapour concentration spans from 0 to 30 ppt: (a) response without gas exposure; (b) response to gas exposure.

370 age at the ASIC chip output is evaluated from the simulation  
 371 results to be  $v_n = 33 \mu\text{V}$ . Considering a RMS signal output  
 372 of 3.3 V the signal-to-noise ratio is

373 
$$\text{SNR} = 20 \log \left( \frac{3.3}{33\mu} \right) = 100 \text{ dB}$$

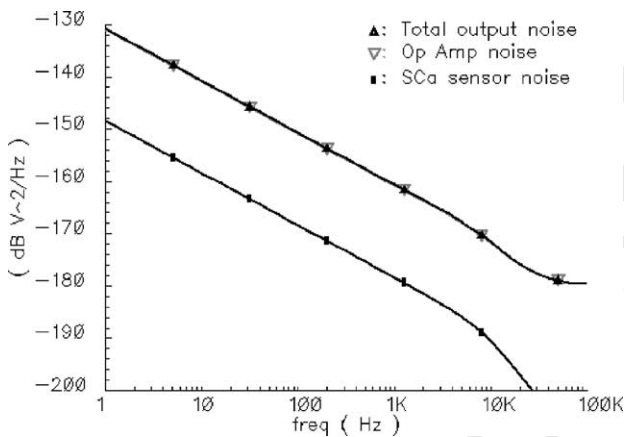


Fig. 15. Noise power spectral density at the ratiometric circuit output and noise contributions of the active sensor and the operational amplifier CFOA23.

374 **4. Conclusions**

375 A novel smart ratiometric ASIC chip has been designed  
 376 for gas sensing applications and fabricated using a standard  
 377 CMOS process. Simulations have shown that the ratiometric  
 378 configuration shows superior performance when compared to  
 379 conventional resistive polymer devices. Its characteristics of  
 380 pulsed-mode operation to prevent polarisation effects/voltage  
 381 induced drifting, and on-chip compensation of temperature and  
 382 humidity variations, are considered to be crucial features for  
 383 the development of an accurate low-cost, palm-top gas monitor.  
 384

385 **Acknowledgements**

386 The authors express their gratitude to Steve Mattheus  
 387 and Greta Milczanowska, from IMEC, Belgium, for their  
 388 valuable help and advice for the testing and verification of  
 389 the design. The support provided through Europractice by  
 390 Dr. Stephen Bell, from Rutherford Appleton Laboratory, is  
 391 also appreciated. Nicola Ulivieri acknowledges Exchange  
 392 and Fellowship Programme of NOSE II (Second Network  
 393 of Excellence on Artificial Olfactory Sensing) for financial  
 394 support.

395 **References**

- 396 [1] M. Cole, J.W. Gardner, J.A. Covington, D. Fife, C.Y. Kwok, J.E.  
397 Brignell, P.N. Bartlett, Active bridge polymeric resistive device for  
398 vapour sensing, *Eurosensors XIV*, W2P41, (Bio)chem. Sens. III  
399 (2000) 895–898.
- 400 [2] J.W. Gardner, M. Vidic, P. Ingleby, A.C. Pike, J.E. Brignell, P. Scivier,  
401 P.N. Bartlett, A.J. Duke, J.M. Elliot, Response of a poly(pyrrole)  
402 resistive micro-bridge to ethanol vapour, *Sens. Actuators B* 48 (1998)  
403 289–295.
- 404 [3] M. Cole, J.W. Gardner, A.W.Y. Lim, P.K. Scivier, J.E. Brignell,  
405 Polymeric resistive bridge gas sensor array driven by a standard cell  
406 CMOS current drive chip, *Sens. Actuators B* 58 (1999) 518–525.
- 407 [4] M. Cole, J.W. Gardner, P.N. Bartlett, Low-drift odour and vapour  
408 ratiometric resistive elements for analogue CMOS smart sensors,  
409 in: J.R. Stetter, W.R. Penrose (Eds.), *Proceedings of the Artificial*  
410 *Chemical Sensing: Olfaction and the Electronic Nose (ISOEN 2001)*,  
411 vol. 15, The Electrochemical Society Inc., USA, 2001, pp. 117–120.
- 412 [5] M. Cole, N. Ulivieri, J. García-Guzmán, J.W. Gardner, Para-  
413 metric model of a polymeric chemoresistor for use in  
414 smart sensor design and simulation, submitted for publication.  
415 <http://www.eng.warwick.ac.uk/srl>.
- 416 [6] P. Bruschi, A. Nannini, B. Neri, Vapour and gas sensing by noise  
417 measurements on polymeric balanced bridge microstructures, *Sens.*  
418 *Actuators B* 24–25 (1995) 429–432.
- 419 [7] J.V. Hattfield, P. Neaves, P.J. Hicks, K. Persaud, P. Travers, Towards  
420 an integrated electronic nose using conducting polymer sensors, *Sens.*  
421 *Actuators B* 18–19 (1994) 221–228.
- 422 [8] S.M. Briglin, M.S. Freund, P. Tokumaru, N.S. Lewis, Exploitation  
423 of spatiotemporal information and geometric optimisation of signal/  
424 noise performance using arrays of carbon black-polymer com-  
425 posite vapor detectors, *Sens. Actuators B* 82 (2002) 54–74.

426 **Biographies**

427 *Jesús García-Guzmán* graduated in Mechanical and Electrical Engineer-  
428 ing from the Universidad Veracruzana (Veracruz, Mexico) in 1978. He  
429 received his MSc degree in Higher Education, with honours, from the  
430 ICESS (Mexico) in 1997 and MSc degree in Advanced Engineering,  
431 with distinction, from the University of Warwick (UK) in 1999. He is a  
Lecturer in the Faculty of Engineering at the Universidad Veracruzana

(Xalapa, Mexico). Currently he is completing work on a PhD project at  
the Sensors Research Laboratory of the University of Warwick, where  
his main research interests are in the areas of analogue integrated circuit  
design, sensor interfacing and smart circuitry.

*Nicola Ulivieri* received his Laurea degree in Telecommunication Engi-  
neering at the University of Siena in 1999. He is currently a PhD student  
in Information Engineering (Electronics) at the University of Siena. In  
2002 he spent a 6 months period at the School of Engineering of the  
University of Warwick to develop a Cadence model for chemoresistors  
gas sensors and to collaborate to an ASIC chip layout design. His main  
research activity is related to the development of laboratory electronic  
noses based on metal oxide sensors and QCM sensors. Recently, his  
interests were also devoted to integrated analogue and mixed signal  
electronics design and smart sensors development.

*Marina Cole* (BSc, PhD, MIEEE), received his BSc degree from the  
University of Montenegro (Yugoslavia) and the PhD from Coventry  
University (UK). She joined the School of Engineering at Warwick Uni-  
versity in 1996 as a postdoctoral research assistant and in 1998 she was  
appointed to a lectureship in electronic engineering. Her main research in-  
terests are integrated silicon-based sensors, SAW-based sensors, analogue  
and mixed signal ASICs, smart sensors, actuators and microsystems.

*Julian W. Gardner* (BSc, PhD, DSc, CEng, FIEE, SMIEEE), joined the  
School of Engineering at Warwick in 1987. His research interests are  
microsensors, microsystems technology, electronic noses, intelligent sen-  
sors and multivariate data processing methods. He has previously spent  
5 years in industry working first at AEA Technology Ltd. and later at  
Molins Advanced Technology Unit on Instrumentation. At Molins he de-  
veloped a novel opto-electronic sensor that has been packaged in the  
UK and US for implementation on high speed packaging machinery. In  
1989 he received his Esso Centenary Education Award sponsored by the  
Royal Society and Fellowship of Engineering to pursue his research in-  
terests. He has published over 300 technical papers and is an author of  
six books in Nanotechnology (1991), *Electronic Noses* (1992), *Microsen-  
sors* (1994), *Electronic Noses* (1999), and *MEMS* (2001). He was an  
Alexander von Humboldt Fellowship in Germany in 1994. He currently  
heads the Sensors Research Laboratory in the Centre for Nanotechnology  
and Microengineering at Warwick University, where he is Professor of  
Electronic Engineering.